

See discussions, stats, and author profiles for this publication at: <https://www.researchgate.net/publication/279727217>

# Diffusion of Small Solute Particles in Viscous Liquids: Cage Diffusion, a Result of Decoupling of Solute–Solvent Dynamics, Leads to Amplification of Solute Diffusion

ARTICLE in THE JOURNAL OF PHYSICAL CHEMISTRY B · JULY 2015

Impact Factor: 3.3 · DOI: 10.1021/acs.jpcc.5b03034 · Source: PubMed

---

READS

43

5 AUTHORS, INCLUDING:



[Sayantan Acharya](#)

CSIR - National Chemical Laboratory, Pune

2 PUBLICATIONS 0 CITATIONS

SEE PROFILE



[Manoj Kumar Nandi](#)

CSIR - National Chemical Laboratory, Pune

3 PUBLICATIONS 2 CITATIONS

SEE PROFILE



[Sarika Bhattacharyya](#)

CSIR - National Chemical Laboratory, Pune

36 PUBLICATIONS 694 CITATIONS

SEE PROFILE

# **Diffusion of Small Solute Particles in Viscous Liquids: Cage Diffusion, a Result of Decoupling of Solute-Solvent Dynamics, Leads to Amplification of Solute Diffusion**

Sayantan Acharya, Manoj K. Nandi, Arkajit Mandal, Sucharita Sarkar, and  
Sarika Maitra Bhattacharyya\*

*Polymer Science and Engineering Department, National Chemical Laboratory,  
Pune-411008, India. Tel. No. - +91 (020) 25903144, Fax No. - +91 (020) 25902636*

E-mail: [mb.sarika@ncl.res.in](mailto:mb.sarika@ncl.res.in)

## Abstract

We study the diffusion of small solute particles through solvent keeping the solute-solvent interaction repulsive and varying the solvent properties. The study involves computer simulations, development of a new model to describe diffusion of small solutes in a solvent and also mode coupling theory (MCT) calculations. In a viscous solvent a small solute diffuses via coupling to the solvent hydrodynamic modes and also through the transient cages formed by the solvent. The model developed can estimate the independent contributions from these two different channels of diffusion. While the solute diffusion in all the systems show an amplification, the degree of it increases with solvent viscosity. The model correctly predicts that when the solvent viscosity is high the solute primarily diffuses by exploiting the solvent cages. In such a scenario the MCT diffusion performed for a static solvent provides a correct estimation of the cage diffusion.

**Keywords** Stokes-Einstein Equation, Repulsive Interaction, Mode Coupling Theory, Oscillator Model.

# 1 Introduction

The study of transport, in simple and complex fluids and also biological systems, has always been an extremely important field of research. Many a times the understanding derived from simple systems helps us understand the more complex ones. Amongst the transport properties, the self-diffusion coefficient is the one, studied extensively both in experimental and theoretical work. Phenomenon such as adsorption, separation, catalytic activity etc, are found to be dependent on self diffusion.<sup>1-3</sup> Self diffusion in simple liquids is usually described by the Stokes-Einstein (SE) relation which was first derived by Einstein to address the diffusion of a “Stokes” particle undergoing Brownian dynamics.<sup>4-6</sup> The equation predicts an inverse dependence of the solute diffusion,  $D$ , on the solvent viscosity,  $\eta$ , and solute radius  $R$ .

$$D = \frac{k_B T}{s \pi \eta R}, \quad (1)$$

where  $s = 6$  for stick boundary condition and 4 for slip boundary condition. This powerful equation although derived in the hydrodynamic limit where the solvent appears to be a continuum to the solute, is found to be valid even at microscopic levels where the solute and the solvent are of similar sizes. According to the mode coupling theory (MCT) since both the friction which describes the diffusion and the viscosity are determined by the solvent structures and its dynamics thus the relation between them is valid even at the microscopic level.<sup>7</sup> According to this study as long as the solute friction is determined primarily by the solvent dynamics the SE relation will hold.

However, even for simple liquids the SE relationship in some cases is found to breakdown.<sup>7-27</sup> Many a times the breakdown marks changes appearing in the system and its transport mechanism. In case of supercooled liquids the breakdown of this relationship is connected to the system developing different dynamic domains and becoming heterogeneous.<sup>9-15</sup> The diffusion of small solute particle is also known to show a deviation from the SE relation.<sup>16-24</sup> Different

experimental, theoretical and computational simulation studies attribute this deviation to apparently different phenomena. In some cases an empirical modification of the SE relation, assuming a fractional viscosity dependence, is used to explain the deviation.<sup>16–18,20,21</sup> In another study an effective radius, determined by the solute-solvent size ratio is assumed to provide the correct results.<sup>26</sup> However, the origin of the micro-viscosity/fractional viscosity and the effective radius, are not well understood. Bhattacharyya and Bagchi have shown that the small solutes have faster dynamics than the solvent.<sup>24</sup> This leads to the decoupling between the solute and the solvent. In such a scenario although the solvent viscosity is primarily determined by the solvent structure and its dynamics the solute friction/diffusion due to the decoupling becomes independent of the same. This decoupling leads to the lowering of friction giving rise to larger diffusion<sup>24</sup> which leads to the breakdown of SE relation. In another study it was shown that for smaller solute this deviation becomes stronger at higher density.<sup>25</sup> Sharma and Yashonath have argued that small solutes explore the solvent cages and when the interaction between the solute and the solvent is attractive, for certain solute sizes there is a force balance which leads to faster diffusion of the solute through the cage.<sup>27–30</sup> This effect which is known as Levitation effect is responsible for the breakdown of the SE relation.<sup>27</sup> From all these seemingly contradictory results it is difficult to conclude what change in the transport phenomena leads to the breakdown of SE relation for small solutes.

In this article we study the diffusion of small solute particles over a range of solute diameters. The solvent properties are also varied over a large range to explore solvents with both high and low viscosity. Earlier studies have shown that diffusion in strikingly different medium like diffusion in solid porous Zeolites<sup>28</sup> and viscous medium show similar characteristics.<sup>31</sup> The levitation effect arising in the porous system, due to the cage diffusion is also present in the latter. This similarity has been explained in terms of presence of transient solvent cages in a solute-solvent system.<sup>31</sup> Note that when the dynamics of the solute is faster than the solvent, for a certain time, the latter will appear like a solid to the former. Only in this limit

the solute can explore these solvent cages. Thus in a solute-solvent system there exists two different modes of diffusion, the viscous diffusion and the cage diffusion. We develop a model of solute diffusion which describes the diffusion of the solute when it is coupled to the solvent hydrodynamic modes and also can diffuse through the solvent cages. Since the cage diffusion is a phenomena where the solvent appears like a solid to the solute we model this using the concepts of Oscillator model proposed by Bhatia and coworkers to describe the diffusion of a particle through a solid cylindrical nanopore.<sup>32-34</sup> Oscillator model has successfully described the size dependence of solute diffusion both for attractive and repulsive interactions.<sup>32,33</sup>

Fitting our model to the simulation results we can estimate the contribution from the viscous diffusion and the diffusion due to cage exploration. In this study we show that even for repulsive solute-solvent interaction the cage diffusion is responsible for the amplified solute diffusion. However the study further shows that the exploration of the solvent cage is only possible when the solvent viscosity is high and there is a decoupling between the solute and the solvent dynamics. Thus the study bridges the gap between studies<sup>24,27</sup> presenting apparently contradictory explanations of the origin of the breakdown of the SE relation for small solutes.

The next section contains Simulation Details. Section 3 contains the Results and Discussion followed by Conclusion in section 4.

## 2 Simulation Details

In this work we perform an equilibrium Molecular Dynamics simulation with an atomistic model where particle type ‘i’ is interacting with particle type ‘j’ with truncated and shifted Lennard-Jones (LJ) pair potentials, given by

$$\Phi_{ij}(r_{ij}) = \Phi_{ij}^{LJ}(r_i, \sigma_{ij}, \epsilon_{ij} - \Phi_{ij}^{LJ}(r_{ij}^{(c)}, \sigma_{ij}, \epsilon_{ij})), r_{ij} \leq r_{ij}^c \quad (2)$$

$$= 0, r_{ij} > r_{ij}^c \quad (3)$$

Where  $\Phi_{ij}^{LJ}(r_{ij}, \sigma_{ij}, \epsilon_{ij}) = 4\epsilon_{ij}[(\frac{\sigma_{ij}}{r_{ij}})^{12} - (\frac{\sigma_{ij}}{r_{ij}})^6]$ ,  $r_{ij}$  is the distance between pairs,  $r_{ij}^c = 2^{\frac{1}{6}}\sigma_{ij}$  for Weeks-Chandler-Andersen (WCA) system<sup>35</sup> and  $r_{ij}^c = 2.5\sigma_{ij}$  for LJ system. Here  $i, j = 1, 2$ , where 1 refers to solvent and 2 refers to solute. For all the systems we consider that the interaction between the solvent and the solute has a soft core which allows inter-penetration between solute-solvent pair (see Table 1).

We take a system with 1000 particles where 10 of them are solute and rest are solvent. We study four different systems varying the interaction potential, solvent mass and the interspecies interaction length given in the Table 1.

NPT simulations are carried in a cubic box at a reduced temperature  $T^*=1.663$ , and reduced pressure 7. To avoid crystallization, system 2 is simulated at  $T^*=2$ . Simulations are performed with time step of  $0.001\tau$ , where  $\tau = \sqrt{\frac{m\sigma_{11}^2}{\epsilon}}$ . In this study, length and temperature are given in the units of  $\sigma_{11}$  and  $\frac{k_B T}{\epsilon}$ . All the above mentioned systems are equilibrated for 1-2ns followed by a production run of 4ns. Systems with larger mass are simulated with longer equilibration time. The molecular dynamics simulations are carried out using LAMMPS package.<sup>36</sup>

### 3 Results and Discussion

We find that the solutes in all the systems studied here show an amplification of diffusion. However since the solvent viscosity shows a large variation, in order to do a comparative study of the degree of amplification in different systems, we use the SE relation as a measure. The solvent diffusion at high temperatures is known to be coupled to the viscosity.<sup>24,25</sup> Thus in

eq 1 by replacing the  $\eta$  value by the solvent diffusion we can write,

$$\frac{D_2}{D_1} = \frac{\sigma_{11}}{\sigma_{22}}, \quad (4)$$

where  $D_2$  is the solute diffusion,  $D_1$  is solvent diffusion,  $\sigma_{11}$  and  $\sigma_{22}$  are the solvent and solute diameters respectively. In 1 we plot  $\frac{D_2}{D_1}$  as a function of  $\frac{1}{\sigma_{22}}$  (as  $\sigma_{11} = 1$ ).

We find that the deviation from the SE prediction increases with the solvent viscosity. The origin of this is not fully understood. As mentioned earlier, different studies have attributed this large diffusion to apparently different phenomena. In one case it is the decoupling of solute-solvent motion<sup>24</sup> and in other case it is the Levitation effect which was found to be responsible for it.<sup>27</sup> The later is known to arise from solute exploring solvent cages. As mentioned in the Introduction when the solute dynamics is orders of magnitude faster than the solvent in the initial time the solvent appears like a solid to the solute. This allows the solute to explore the solvent cages. However when the decoupling in dynamics is not strong in later times the solute might also be able to explore the viscous properties of the solvent. Thus a small solute diffusing in a viscous system has two different contribution to its diffusion. In simulation studies of solute diffusion it is not possible to individually make an estimation of these two independent components. In order to decouple these two contributions to solute diffusion we propose a model where the contribution from the solvent hydrodynamic modes is assumed to be given by the SE relation as we assume in this regime the solute the solvent dynamics are coupled and the cage diffusion is modeled using Oscillator Model (OM)<sup>32,33</sup> which was developed for studying diffusion through a nanoporous solid.

### 3.1 Oscillator Model

According to the Oscillator model of Bhatia and coworkers,<sup>32-34</sup> particle diffusing through a cylindrical nanopore at low particle density oscillates along the plane perpendicular to the



tube axis. Here, the transport diffusivity of the particle of mass ‘m’ at temperature T is given by,  $D_t = \frac{k_B T}{m} \langle \tau \rangle$ , where  $\langle \tau \rangle$  is the average oscillation time of the trajectory in the nanopore at temperature, T. The bigger the pore, the longer will be the time of oscillation and the collision frequency will reduce. This in turn will reduce the rate of axial momentum loss of the confined particle thus leading to higher diffusion along the pore axis. Following the same logic a similar effect of increase of diffusion value can be obtained by keeping the pore radius fixed and reducing the particle size. Using Hamiltonian equation of motion the oscillation time for a particle moving in a radial potential function can be written as,<sup>33</sup>

$$\tau(r, p_r, p_\theta) = 2m \int_{r_{c0}(r, p_r, p_\theta)}^{r_{c1}(r, p_r, p_\theta)} \frac{dr'}{p_r(r', r, p_r, p_\theta)}. \quad (5)$$

Where  $r_{c0}$  is the radial position at the point closest to center, the point of reflection near the wall is  $r_{c1}$  and the radial momentum profile,  $p_r(r', r, p_r, p_\theta)$ , can be written as,

$$p_r(r', r, p_r, p_\theta) = \left[ 2m \left[ \Phi_{fs}(r) - \Phi_{fs}(r') \right] + p_r^2(r) + \left( \frac{p_\theta}{r} \right)^2 \left( 1 - \frac{r^2}{r'^2} \right) \right]^{\frac{1}{2}}. \quad (6)$$

when  $\Phi_{fs}(r)$  is the radial potential field. We get  $r_{c0}$  and  $r_{c1}$  value by solving  $p_r(r', r, p_r, p_\theta) = 0$ .

Averaging the oscillation time  $\tau$  over the canonical distribution of  $r, p_r$  and  $p_\theta$ , the low-density transport coefficient in the presence of a one-dimensional potential field in a cylindrical pore is given by,

$$D = \frac{2}{\pi m Q} \int_0^{r^{ph}} dr \int_0^\infty e^{-\frac{\beta p_r^2}{2m}} dp_r \int_0^\infty e^{-\frac{\beta p_\theta^2}{2mr^2}} dp_\theta \int_{r_{c0}(r, p_r, p_\theta)}^{r_{ph}} \frac{dr'}{p_r(r', r, p_r, p_\theta)} \quad (7)$$

where  $p_r$  and  $p_\theta$  are momentum parameters and  $Q = \int_0^\infty r e^{\beta \Phi_{fs}(r)} dr$ .

It was shown that for hard spheres (HS) systems eq 7 reduces to the classical Knudsen

model,<sup>32,33</sup>

$$D^{Knudsen} = \frac{4r_{ph}}{3} \sqrt{\frac{2k_B T}{\pi m}}, \quad (8)$$

where  $r_{ph}$  is the maximum displacement possible from the center of the pore to the pore wall. We calculate the diffusion coefficients  $D^{WCA}$  and  $D^{HS}$  as obtained from the OM where the interaction between the particle and the nanopore is given by WCA and hard sphere(HS) potentials, respectively. The calculations were done for a fixed size of the nanopore,  $r_{pore}$  and varying the size of the diffusing particle,  $\sigma_{22}$ . We compare  $D^{WCA}$  and  $D^{HS}$  at temperature 1.663 with the classical Knudsen model (2). Although all three models predict the diffusive to be linear with  $r_{ph}$ , ( $r_{ph} = r_{pore} - \frac{\sigma_{22}}{2}$ ),  $D^{Knudsen}$  shows slightly stronger  $r_{ph}$  dependence whereas the  $r_{ph}$  dependence of  $D^{WCA}$  and  $D^{HS}$  are similar in nature. The diffusion values for the WCA systems are a bit lower because the length-scale of the WCA potential is larger than the hard sphere (HS) potential making the pore narrower (2).

### 3.2 Our Model

As discussed before, in a solute-solvent system the solvents form transient cages through which a small solute can diffuse.<sup>31,37</sup> The neck of the cage can be considered as an nanopore. The diffusion of a particle through a neck is similar to that along the pore axis. Thus the Oscillator Model can be used to understand the diffusion of a solute through the transient solvent cages.

However unlike a fixed radius of a nanopore the solvent cages have a distribution of neck sizes.<sup>31</sup> The distribution can be approximated by a Gaussian function,  $g(r_{neck}) = \frac{1}{h\sqrt{2\pi}} \exp -\frac{1}{2}(\frac{r_{neck}-\nu}{h})^2$ , where  $g_{neck}$  is the distribution of neck size in the solution.  $r_{neck}$  is the radius of the neck formed by the solvent particles.  $\nu$  is the mean position and  $h$  is the full width at half maxima of the distribution. From earlier studies we find that  $\nu = 0.2\sigma_{11}$  and  $h = 0.0583\sigma_{11}$ .<sup>31</sup> For a

repulsive solute-solvent interaction (given by WCA potential) the diffusion of solute through the solvent cages, incorporating the neck size distribution of these cages can be written as,

$$D_{neck}^{WCA} = \int g(r_{neck}) D^{WCA} dr_{neck} \quad (9)$$

$$= c \int g(r_{neck}) r_{ph}(r_{neck}) dr_{neck}, \quad (10)$$

The second equality is written assuming linear dependence of  $D^{WCA}$  on  $r_{ph}$  and obtaining the slope ‘c’ from 2. The  $r_{ph}$  is defined as a function of  $r_{neck}$ , which can be written as,  $r_{ph} = r_{neck} + r_{pene} - \frac{\sigma_{22}}{2}$ . Note that in our model  $\sigma_{12}$  is smaller than that predicted by additive Lorentz-Berthelot rule<sup>38</sup> (see Table 1), thus the solute can partially penetrate a solvent particle. The inter-penetration distance is given by  $r_{pene} = \frac{\sigma_{11} + \sigma_{22}}{2} - (0.171 + \sigma_{22})$ . As shown in the inset of 2 presence of the distribution of neck sizes although predicts a small deviation of the  $D_{neck}^{WCA}$  from that predicted by the OM the behavior remains similar.

We describe the diffusion of a solute as a sum of that predicted by the SE relation and the diffusion through transient solvent cages. Note that in the rest of the article the neck diffusion and diffusion through the cage will be used synonymously. The total diffusion can be written as,

$$D_{tot} = D_{SE} + P D_{neck}^{WCA} = D_{SE} + D_{neck}, \quad (11)$$

P is the average neck population that a solute particle encounters in the timescale of its Stokes-Einstein diffusion. Replacing the expression of  $D_{neck}^{WCA}$  (given in eq 10 ) in eq 11 the  $D_{tot}$  can be written as,

$$D_{tot} = \frac{K_B T}{3\pi\eta\sigma_{22}} + P c \int g(r_{neck}) r_{ph}(r_{neck}) dr_{neck}. \quad (12)$$

Considering the solvent to follow SE relation eq 12 can be rewritten as,

$$D_{tot} = D_1 \frac{\sigma_{11}}{\sigma_{22}} + Pc \int g(r_{neck}) r_{ph}(r_{neck}) dr_{neck}. \quad (13)$$

In the above equation the neck population explored by the solute,  $P$ , has been kept as a fitting parameter. Fitting this equation to the simulation results as a function of solute size should give us an estimation of  $P$ . Note that systems 2, 3 and 4 show a strong amplification of solute diffusion, thus the diffusion in these systems cannot be explained completely via SE relation ( $D_{SE}$ ) and should be primarily given by diffusion due to neck exploration,  $D_{neck}$ . However  $D_{neck}$  shows a linear  $\sigma_{22}$  dependence (inset, 2) whereas  $D_{tot}$  is a nonlinear function of  $\sigma_{22}$  (3). Thus the model predicts that in order to fit eq 13 to the simulation data,  $P$  should have a dependence on the solute size. We note that a smaller solute which can diffuse faster should explore larger number of cages compared to a bigger solute, thus as predicted by our model, the explored neck population should indeed be dependent on the size of the solute. To incorporate this dependence we consider the population to be a function of  $D_{SE}$  and  $D_{neck}^{WCA}$ . Thus we write it as,

$$P = \alpha \left[ D_1 \frac{\sigma_{11}}{\sigma_{22}} + \int g(r_{neck}) r_{ph}(r_{neck}) dr_{neck} \right], \quad (14)$$

where  $\alpha$  is the proportionality constant.

Replacing eq 14 in eq 13 and using  $\alpha$  as a fitting parameter we compare the simulation results with the diffusion values as predicted by our model. We find that our model provides a good description of the  $\sigma_{22}$  dependence of the diffusion for all the systems studied here (3). Next we analyze the contributions from the different components of diffusion,  $D_{SE}$  and  $D_{neck}$  for the different systems as predicted by the model. For system 1 which is less viscous (see Table 2) the larger solute particles diffuse via coupling to solvent dynamics and thus follow SE behavior and the diffusion is given primarily via  $D_{SE}$ . However for smaller solutes

both the modes of diffusion are active with the neck contributing little more as the solute size is decreased (Fig. 3a). Note that this system shows a weak deviation from SE behavior (1). For system 2, 3 and 4 where the solvent viscosity is quite high (see Table 2), the model predicts that the diffusion, specially for smaller solute particles take place primarily via  $D_{neck}$  (Fig. 3b,3c,3d),  $D_{SE}$  has a negligible contribution. The viscosity here has two-fold effects. A system with high viscosity has slower moving solvent thus reducing the motion of the solute which is coupled to it. However, high solvent viscosity and a diffusing solute implies a decoupling between solute-solvent dynamics where the solvent appears like a solid to the solute with long lived transient cages. In this limit the solute diffusion mimics the diffusion through a porous medium and depends only on the static structure of the solvent. This is precisely what we observe when we compare diffusion values of systems 1, 3, and 4 (see 4) where the diffusion values for system 3 and 4 are almost independent of the solvent dynamics. Note that the dynamics of the solvent in system 3 when compared to system 4 is faster by about a factor of four, whereas the solute dynamics remains same (see Table 2). The observation that diffusion values grow with the growth of the neck diffusion is similar to that reported by Sharma and Yashonath although for an attractive solute-solvent interaction.<sup>27</sup>

### 3.3 Mode Coupling Theory Prediction

As mentioned earlier according to the study based on MCT calculation it was shown that the decoupling between solute-solvent motion leads to breakdown of Stokes-Einstein prediction.<sup>24</sup> Our present study also reveals that this decoupling is essential for exploration of solvent cages which eventually leads to the breakdown of SE relation. In an earlier work involving some of us we have shown that MCT calculations can explain the Levitation dynamics of small solute, even describing the non-monotonic solute size dependence of diffusion for an attractive solute-solvent interaction.<sup>37</sup> Given the success of MCT in earlier studies it is impetus to do a MCT calculations for our present systems.

According to MCT the diffusion coefficient of a tagged solute particle can be written as,<sup>39</sup>

$$D_{MCT} = k_B T / m_2 \Gamma(z = 0). \quad (15)$$

Here  $\Gamma(z)$  is the frequency dependent friction. Due to difference in timescale the friction term is divided into two parts, the short time part arises from the binary friction ( $\Gamma_B(z)$ ) and the long time part ( $\Gamma_R(z)$ ) comes from the repetitive collisions which are correlated,<sup>39</sup>

$$\Gamma^{ij}(z) \simeq \Gamma_B^{ij}(z) + \Gamma_R^{ij}(z). \quad (16)$$

It has been earlier shown that for solutes having same size or smaller than the solvent the longtime part is dominated by the density contribution.<sup>24</sup> However mode-coupling calculations have further predicted that the decoupling of the solute motion from the solvent dynamics leads to the breakdown of the SE relation.<sup>24</sup> When there is a complete decoupling between the solute-solvent dynamics the only contribution to the solute friction primarily comes from binary component. Amongst the systems that we have studied here we find that diffusion in the systems with higher viscosity (system 2, 3 and 4) takes place primarily through neck diffusion (5). Thus for these systems we can consider a complete decoupling between the solute-solvent dynamics. The diffusion value for these systems as predicted by MCT can be written as,

$$D_{MCT} = k_B T / m_2 \Gamma_B(z = 0), \quad (17)$$

where,  $\Gamma_B(t) = \omega_{012}^2 \exp(-\frac{t^2}{\tau_\zeta^2})$ , where  $\omega_{012}^2$  is Einstein frequency of the solute in presence of the solvent. It is expressed as,

$$\omega_{012}^2 = \frac{\rho}{3m_2} \int d\mathbf{r} g_{12}(\mathbf{r}) \nabla^2 \Phi_{12}(\mathbf{r}), \quad (18)$$

here  $g_{12}(\mathbf{r})$  is the radial distribution function and  $\Phi_{12}(\mathbf{r})$  is the inter atomic potential of the solute-solvent pair.<sup>24</sup> In the expression of  $\Gamma_B(t)$ , the relaxation timescale,  $\tau_\zeta$ , is determined

from the second derivative of  $\Gamma_B(t = 0)$ ,<sup>39</sup>

$$\begin{aligned} \frac{\omega_{012}^2}{\tau_\zeta^2} = & \frac{\rho}{6m_2\mu} \int d\mathbf{r} (\nabla^\alpha \nabla^\beta \Phi_{12}(\mathbf{r})) g_{12}(\mathbf{r}) (\nabla^\alpha \nabla^\beta \Phi_{12}(\mathbf{r})) + \\ & \frac{1}{6\rho} \int [d\mathbf{q}/(2\pi)^3] \gamma_d^{\alpha\beta}(\mathbf{q}) (S(q) - 1) \gamma_d^{\alpha\beta}(\mathbf{q}), \end{aligned} \quad (19)$$

here  $S(q)$  is the static structure factor of the solvent,  $\mu$  is the reduced mass of the solute-solvent pair.  $\gamma_d^{\alpha\beta}(\mathbf{q})$  is combination of the second moments of transverse and longitudinal current correlation function,  $\gamma_d^t(\mathbf{q})$  and  $\gamma_d^l(\mathbf{q})$ , respectively and it is given by,

$$\begin{aligned} \gamma_d^{\alpha\beta}(\mathbf{q}) = & -\left(\frac{\rho}{m_2}\right) \int d\mathbf{r} \exp(-i\mathbf{q} \cdot \mathbf{r}) g_{12}(\mathbf{r}) \nabla^\alpha \nabla^\beta \Phi_{12}(\mathbf{r}) \\ = & \hat{q}^\alpha \hat{q}^\beta \gamma_d^l(\mathbf{q}) + (\delta_{\alpha\beta} - \hat{q}^\alpha \hat{q}^\beta) \gamma_d^t(\mathbf{q}). \end{aligned} \quad (20)$$

Here,  $\gamma_d^l(\mathbf{q}) = \gamma_d^{zz}(\mathbf{q})$  and  $\gamma_d^t(\mathbf{q}) = \gamma_d^{xx}(\mathbf{q})$ .<sup>39</sup>

The MCT prediction for system 2, 3 and 4 are plotted in 5 along with the simulation results. Note that in this calculation the solvent is considered to be static and only its static structural information is required for the calculation of the friction. Our calculation shows that the binary diffusion although slightly overestimates, can explain both the simulation results and the predicted neck diffusion. The marginal overestimation is due to the absence of the density term which has a small contribution to friction. Thus we show that a decoupling between solute and solvent dynamics is essential for the solute to explore the solvent cages and in that case the binary component of the MCT diffusion value can predict the contribution coming from neck diffusion. The success of MCT also implies that in its present framework it can also describe the diffusion through porous medium.

## 4 Conclusions

In this article we present our study of diffusion of small solutes in solvents by varying the size of the solute and also by varying the solvent parameters. The difference between a diffusion of a small and a large solute is that small solutes are known to not only diffuse by being coupled to the hydrodynamic modes of the solvent, which involves density fluctuation and also the transverse and longitudinal currents in the solvent, they can also diffuse through the transient solvent cages if the neck of the cage is big enough to allow the solute through it. The diffusion values as obtained from the simulation studies although contain both the components, are unable to differentiate between them. The present study involves both analytical and computational studies. Computer simulations are performed to obtain the diffusion values and a model is developed to independently access the contribution to diffusion from the solvent hydrodynamic modes and that which is coming from the exploration of transient solvent cages. The exploration of transient solvent cages is similar to the diffusion through a porous solid medium. Thus cage diffusion is modeled based on the OM<sup>32-34</sup> originally developed to calculate the diffusion of particles through solid cylindrical nanopores.

In our model using a single fitting parameter, which is proportional to the population of the cage explored by the solutes, we can describe the solute size dependence of four different systems in different viscosity regimes. The model correctly predicts that the solutes which diffuse faster is able to explore larger population of the cages. The model can further predict the different diffusion contributions. We find that the contribution from the two different modes (viscous and cage exploration) depends on the viscosity/dynamics of the solvent as compared to that of the solute and the solute-solvent size ratio. For larger solutes the diffusion is primarily given by  $D_{SE}$ . However as the size of the solutes are decreased the  $D_{SE}$  reduces and  $D_{neck}$  grows. When the viscosity of the solvent is large the solute particles show an amplified diffusion and primarily diffuses through the cage mode. In this regime the solute diffusion becomes independent of the properties of the solvent dynamics and it mimics



the diffusion through a porous medium where the pores are described by the solvent static structure. In these systems we also perform MCT calculation. We show that the binary collisions which depend only on the static structure of the solvent primarily determines the diffusion. Thus similar to the neck diffusion the MCT calculation is performed for a solvent which is static. The results suggest that the present MCT framework with static solvent is capable of explaining diffusion of solute in a porous medium.

Finally we would like to conclude that the previous observations attributing the break down of the SE relation to apparently two different phenomena, the decoupling of solute-solvent motion<sup>24</sup> and the Levitation effect<sup>27</sup> are not contradictory to each other. In this present study we deal with systems where the solute-solvent interactions are always repulsive thus there is no force balance and hence no Levitation effect. However the Levitation effect reported earlier and our present study both rely on the ability of the solute to explore solvent cage. As shown in the present study this is possible when there is a decoupling of the solute-solvent dynamics. Thus for Levitation to help the solute diffuse faster the solute dynamics must decouple from the solvent motion so that the solvent cages appear stationary in the timescale of solute dynamics.

## 5 Author Information

### Corresponding Author\*

Phone: +91-020-25903144. Fax: +91-020-25902636. E-mail:mb.sarika@ncl.res.in.

### Notes

The authors declare no competing financial interest.

## 6 Acknowledgment

We gratefully acknowledge DST India and CSIR (CSC-0129) for financial support for the project. SA thanks DST for providing fellowship. SS thanks Inspire for providing fellowship. SMB thanks S. Yashonath and Arun Yethiraj for fruitful discussions.

## References

- (1) Ferch, H. Zeolites and Clay Minerals as Sorbents and Molecular Sieves. Von R. M. Barrer. Academic Press, London New York 1978. 1. Aufl., VII, 497 S., zahlr. Abb. u. Tab. *Chemie Ingenieur Technik* **1980**, 52, 366
- (2) Lu, Z. X. E., G.Q. *Nanoporous Materials: Science and Engineering*; Imperical College Press: London, 2005
- (3) Yang, R. T. *Adsorbents: Fundamentals and Applications*
- (4) Einstein, A. On the Theory of the Brownian Movement. *A. Ann. Phys.* **1906**, 19, 371
- (5) Einstein, A. New Determination of Molecular Dimensions. *A. Ann. Phys.* **1906**, 19, 289
- (6) Einstein, A. On the Movement of Small Particles Suspended in a Stationary Liquid Demanded by the Molecular Kinetic Theory of Heat. *A. Ann. Phys.* **1906**, 34, 549
- (7) Bhattacharyya, S.; Bagchi, B. Bimodality of the Viscoelastic Response of a Dense Liquid and Comparison with the Frictional Responses at Short Times. *J. Chem. Phys.* **1998**, 109, 7885–7892
- (8) Biswas, R.; Roy, S.; Bagchi, B. Anomalous Ion Diffusion in Dense Dipolar Liquids. *Phys. Rev. Lett.* **1995**, 75, 1098–1101
- (9) Ediger, M. D.; Angell, C. A.; Nagel, S. R. Supercooled Liquids and Glasses. *J. Phys. Chem.* **1996**, 100, 13200–13212
- (10) Wahnström, G. Molecular-Dynamics Study of a Supercooled Two-component Lennard-Jones System. *Phys. Rev. A* **1991**, 44, 3752–3764
- (11) Thirumalai, D.; Mountain, R. D. Activated Dynamics, Loss of Ergodicity, and Transport in Supercooled Liquids. *Phys. Rev. E* **1993**, 47, 479–489

- (12) Cicerone, M. T.; Blackburn, F. R.; Ediger, M. D. How Do Molecules Move Near T<sub>g</sub>? Molecular Rotation of Six Probes in OTerphenyl Across 14 Decades in Time. *J. Chem. Phys.* **1995**, *102*, 471–479
- (13) Cicerone, M. T.; Ediger, M. D. Enhanced Translation of Probe Molecules in Supercooled OTerphenyl: Signature of Spatially Heterogeneous Dynamics? *J. Chem. Phys.* **1996**, *104*, 7210–7218
- (14) Barrat, J.-L.; Roux, J.-N.; Hansen, J.-P. Diffusion, Viscosity and Structural Slowing Down in Soft Sphere Alloys Near the Kinetic Glass Transition. *Chem. Phys.* **1990**, *149*, 197–208
- (15) Roux, J. N.; Barrat, J. L.; Hansen, J. P. Dynamical Diagnostics for the Glass Transition in Soft-sphere Alloys. *J. Phys.: Condens. Matter* **1989**, *1*, 7171
- (16) Chen, S. H.; Davis, H. T.; Evans, D. F. Tracer Diffusion in Polyatomic Liquids. II. *J. Chem. Phys.* **1981**, *75*, 1422–1426
- (17) Evans, D. F.; Tominaga, T.; Davis, H. T. Tracer Diffusion in Polyatomic Liquids. *J. Chem. Phys.* **1981**, *74*, 1298–1305
- (18) Chen, S.-H.; Evans, D. F.; Davis, H. T. Tracer Diffusion in Methanol, 1-Butanol and 1-Octanol From 298 to 433 K. *AIChE Journal* **1983**, *29*, 640–645
- (19) Heuberger, G.; Sillescu, H. Size Dependence of Tracer Diffusion in Supercooled Liquids. *J. Phys. Chem.* **1996**, *100*, 15255–15260
- (20) Pollack, G. L.; Kennan, R. P.; Himm, J. F.; Stump, D. R. Diffusion of Xenon in Liquid Alkanes: Temperature Dependence Measurements with a New Method. Stokes–Einstein and Hard Sphere Theories. *J. Chem. Phys.* **1990**, *92*, 625–630
- (21) Pollack, G. L.; Enyeart, J. J. Atomic Test of the Stokes-Einstein law. II. Diffusion of Xe Through Liquid Hydrocarbons. *Phys. Rev. A* **1985**, *31*, 980–984

- (22) Ould-Kaddour, F.; Barrat, J.-L. Molecular-dynamics Investigation of Tracer Diffusion in a Simple Liquid. *Phys. Rev. A* **1992**, *45*, 2308–2314
- (23) Murarka, R. K.; Bhattacharyya, S.; Bagchi, B. Diffusion of Small Light Particles in a Solvent of Large Massive Molecules. *J. Chem. Phys.* **2002**, *117*, 10730–10738
- (24) Bhattacharyya, S.; Bagchi, B. Anomalous Diffusion of Small Particles in Dense Liquids. *J. Chem. Phys.* **1997**, *106*, 1757–1763
- (25) Bhattacharyya, S.; Bagchi, B. Decoupling of Tracer Diffusion from Viscosity in a Supercooled Liquid Near the Glass Transition. *J. Chem. Phys.* **1997**, *107*, 5852–5862
- (26) Zwanzig, R.; Harrison, A. K. Modifications of the StokesEinstein formula. *J. Chem. Phys.* **1985**, *83*, 5861
- (27) Sharma, M.; Yashonath, S. Breakdown of the StokesEinstein Relationship: Role of Interactions in the Size Dependence of Self-Diffusivity. *J. Phys. Chem. B* **2006**, *110*, 17207–17211
- (28) Yashonath, S.; Santikary, P. Diffusion of Sorbates in Zeolites Y and A: Novel Dependence on Sorbate Size and Strength of Sorbate-Zeolite Interaction. *J. Phys. Chem.* **1994**, *98*, 6368–6376
- (29) Ghorai, P. K.; Yashonath, S. Diffusion Anomaly at Low Temperatures in Confined Systems from the Rare Events Method. *J. Phys. Chem. B* **2004**, *108*, 7098–7101
- (30) Sharma, M.; Yashonath, S. Correction to Breakdown of StokesEinstein Relationship: Role of Interactions in the Size Dependence of Self-Diffusivity. *J. Phys. Chem. B* **2007**, *111*, 7928
- (31) Ghorai, P. K.; Yashonath, S. The StokesEinstein Relationship and the Levitation Effect: Size-Dependent Diffusion Maximum in Dense Fluids and Close-Packed Disordered Solids. *J. Phys. Chem. B* **2005**, *109*, 5824–5835

- (32) Bhatia, S. K.; Jepps, O.; Nicholson, D. Tractable Molecular Theory of Transport of Lennard-Jones Fluids in Nanopores. *J. Chem. Phys.* **2004**, *120*, 4472–4485
- (33) Anil Kumar, A. V.; Bhatia, S. K. Mechanisms Influencing Levitation and the Scaling Laws in Nanopores: Oscillator Model Theory. *J. Phys. Chem. B* **2006**, *110*, 3109–3113
- (34) Jepps, O. G.; Bhatia, S. K.; Searles, D. J. Wall Mediated Transport in Confined Spaces: Exact Theory for Low Density. *Phys. Rev. Lett.* **2003**, *91*, 126102
- (35) Weeks, J. D.; Chandler, D.; Andersen, H. C. Role of Repulsive Forces in Determining the Equilibrium Structure of Simple Liquids. *J. Chem. Phys.* **1971**, *54*, 5237–5247
- (36) Plimpton, S. Fast Parallel Algorithms for Short-Range Molecular Dynamics. *J. Comput. Phys.* **1995**, *117*, 1–19
- (37) Nandi, M. K.; Banerjee, A.; Bhattacharyya, S. M. Non-monotonic Size Dependence of Diffusion and Levitation Effect: A Mode-Coupling Theory Analysis. *J. Chem. Phys.* **2013**, *138*, 124505
- (38) J.S.Rowlinson, *Liquid and Liquid Mixtures*; Butterworths,London,1969
- (39) Sjogren, L.; Sjolander, A. Kinetic Theory of Self-Motion in Monatomic Liquids. *J. Phys. C: Solid State Phys.* **1979**, *12*, 4369

## List of Table

**Table 1:** The parameters used in the model systems, where  $\sigma_{11}, \sigma_{12}$  and  $\sigma_{22}$  are solvent, solute-solvent and solute diameters, respectively,  $\epsilon_{11}, \epsilon_{12}$  and  $\epsilon_{22}$  are interaction parameters for solvent-solvent, solute-solvent and solute-solute pairs respectively which are scaled by  $\epsilon$ . Here for all the systems  $\sigma_{11} = 1, \epsilon_{22} = 0.5$  and we have considered a range of solute radius as,  $\sigma_{22} = 0.073, 0.098, 0.122, 0.171, 0.2, 0.22, 0.244, 0.293, 0.317, 0.366$ . Mixed potential is referred to attractive interaction (LJ) between solvent-solvent and repulsive interaction (WCA) between solute-solvent and solute-solute pairs.  $m_1$  is the solvent mass and  $m_2$  is the solute mass which is 1

sys-Potentials	$\frac{\epsilon_{11}}{\epsilon}$	$\frac{\epsilon_{12}}{\epsilon}$	$m_1$	$\sigma_{12}$
1-WCA	1	1	1	$\sigma_{22} + 0.171$
2-Mixed	3	1	1	$\sigma_{22} + 0.171$
3-Mixed	1	1	10	$\sigma_{22} + 0.171$
4-Mixed	1	1	100	$\sigma_{22} + 0.171$

**Table 2:** Solvent Diffusion values for all the systems. We also present a representative solute diffusion value (for  $\sigma_{22} = 0.073$ ) to show the decoupling of solute-solvent dynamics.

system	$D_1$	$D_2$
1	0.182	6.2
2	0.023	5.4
3	0.0273	5.3
4	0.007	5

## List of Figures

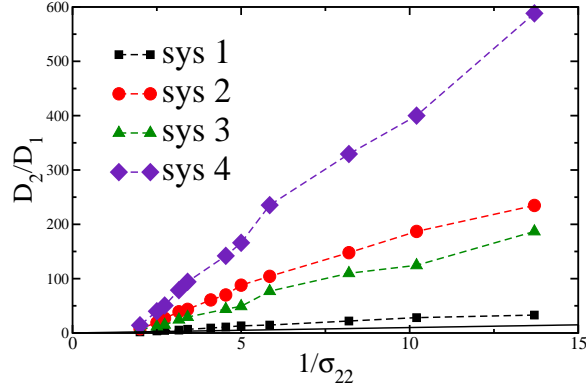


Figure 1:  $D_2/D_1$  values for all the systems as a function of  $1/\sigma_{22}$ . The SE prediction is also plotted for comparison (solid line).

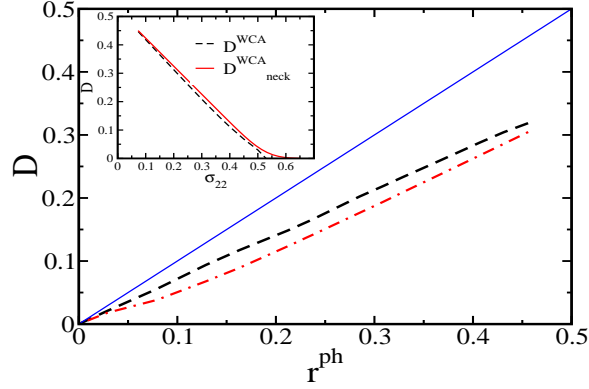


Figure 2: The diffusion values as a function of  $r_{ph}$  as calculated from eq 7 for WCA (dash-dot line,  $D^{WCA}$ ) and HS system (dashed line,  $D^{HS}$ ). We also plot the diffusion values as predicted by the classical Knudsen model (solid line,  $D^{Knudsen}$ ). Inset-Diffusion values as a function of  $\sigma_{22}$  as calculated from eq 7 using WCA potential,  $D^{WCA}$  and from eq 10 where we consider a distribution of neck size,  $D^{WCA}_{neck}$ . The solute size dependence of diffusion before and after the incorporation of the neck size distribution remains similar.



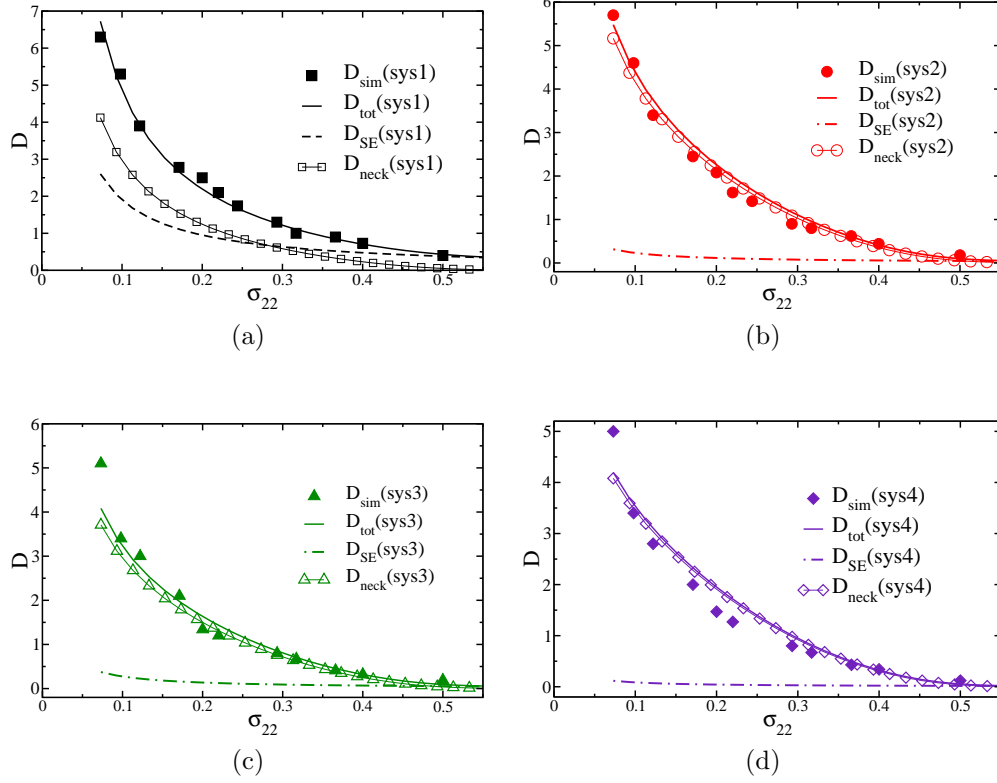


Figure 3:  $D_{tot}$ ,  $D_{SE}$  and  $D_{neck}$  are plotted against  $\sigma_{22}$  for all the systems.  $D_{tot}$  is obtained from fitting eq 13 and 14 to simulated values using  $\alpha$  as a fitting parameter.  $D_{SE}$  and  $D_{neck}$  are the corresponding SE diffusion and neck diffusion as obtained from the model with fitted  $\alpha$  value.

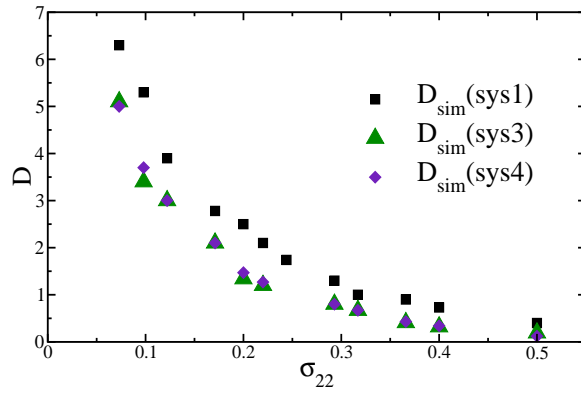


Figure 4: The simulated diffusion values ( $D_{sim}$ ) for the systems 1, 3 and 4.

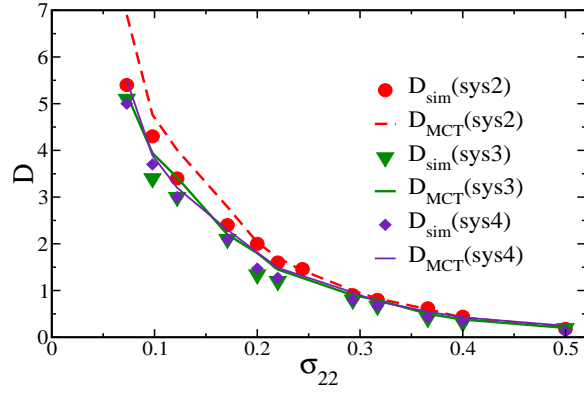


Figure 5:  $D_{sim}$  and  $D_{MCT}$  plotted as a function of  $\sigma_{22}$  for systems 2, 3 and 4.  $D_{MCT}$  is calculated considering only the binary friction.

## Table of contents (TOC)- Graphics

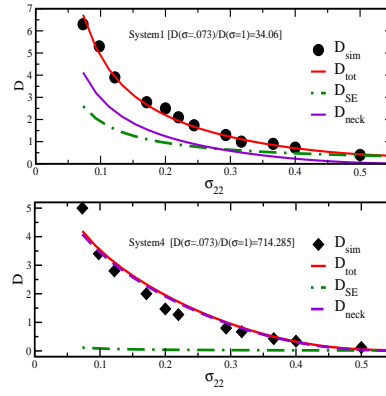


Figure 6: